

# Utrecht University Repository

Title	Tipping mechanisms in a conceptual model of the Atlantic Meridional Overturning Circulation
Authors	Chapman, Ruth; Sinet, Sacha; Ritchie, Paul D. L.
Published in	Weather
Publication Date	2024-10
Link	<a href="https://dspace.library.uu.nl/handle/1874/472579">https://dspace.library.uu.nl/handle/1874/472579</a>
Citation	Chapman, R, Sinet, S & Ritchie, P D L 2024, 'Tipping mechanisms in a conceptual model of the Atlantic Meridional Overturning Circulation', Weather, vol. 79, no. 10, pp. 316-323. <a href="https://doi.org/10.1002/wea.7609">https://doi.org/10.1002/wea.7609</a>
Versions / License	Publisher version
Rights	<a href="https://www.uu.nl/en/university-library/license-and-reuse-conditions">https://www.uu.nl/en/university-library/license-and-reuse-conditions</a>

# Tipping mechanisms in a conceptual model of the Atlantic Meridional Overturning Circulation

Ruth Chapman<sup>1</sup> ,  
Sacha Sinet<sup>2,3</sup>  and  
Paul D. L. Ritchie<sup>1,4</sup> 

<sup>1</sup>Department of Mathematics and Statistics, University of Exeter, UK

<sup>2</sup>Department of Physics, Institute for Marine and Atmospheric Research Utrecht, Utrecht University, the Netherlands

<sup>3</sup>Center for Complex Systems Studies, Utrecht University, the Netherlands

<sup>4</sup>Global Systems Institute, University of Exeter, UK

## Introduction

The global ocean circulation plays a key role in shaping the present day climate by transporting heat, salt and nutrients across the globe. An essential component of this system is the Atlantic Meridional Overturning Circulation (AMOC) (Figure 1a), which is

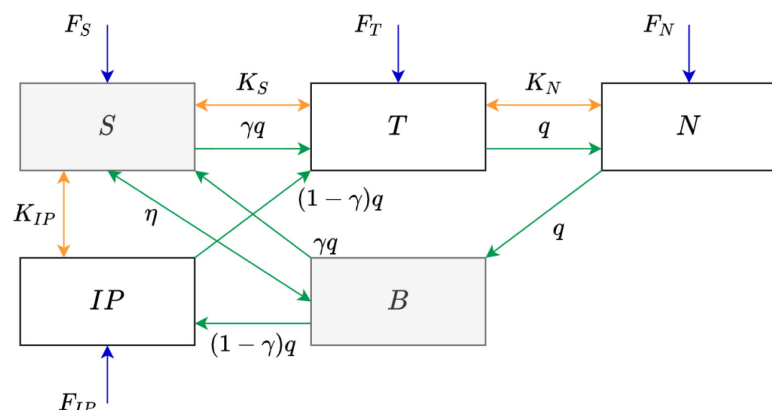
projected to weaken under anthropogenic climate change. Furthermore, the AMOC is classified as a core tipping element of the climate system (Armstrong McKay *et al.*, 2022), suggesting the existence of some critical threshold of forcing, such as global temperature or freshwater input into the North Atlantic. Exceeding this threshold may cause the AMOC to abruptly and/or irreversibly collapse. This collapse could range from a significant weakening to a complete shutdown of the AMOC, which would have important consequences globally. This includes disruptions to precipitation patterns (Bellomo *et al.*, 2021), the global carbon budget (Sarmiento and Le Quéré, 1996) and to the present heat distribution across the globe – especially threatening the relatively mild European climate (Seager *et al.*, 2002; Jackson *et al.*, 2015; van Westen *et al.*, 2024). Additionally, the AMOC has a central position in a network of interacting tipping elements, including the Polar ice sheets (Sinet *et al.*, 2023; Wunderling *et al.*, 2023). Therefore, in a

worst case scenario, an AMOC collapse may mediate cascading tipping phenomena, in which the tipping of one element triggers the tipping of others (Dekker *et al.*, 2018; Klose *et al.*, 2021; Wunderling *et al.*, 2021).

The AMOC is considered as a tipping element due to the presence of a positive feedback loop, known as the salt-advection feedback. Specifically, the sinking of dense surface waters in the North Atlantic region (Figure 1) drives the AMOC. This high density partly results from the relatively cool climate of the Northern Hemisphere but is also widely sustained by the AMOC itself, as the transport of salt from lower to higher latitudes maintains a relatively high salinity in this region. Hence, a strengthening or weakening of the AMOC tends to be amplified by the subsequent salinification or freshening of the North Atlantic, respectively. This salt-advection feedback was first investigated in a simple box model of the AMOC (Stommel, 1961). This model showed that two stable states could coexist for the same level of forcing



(a) AMOC illustration



(b) Five-box AMOC model

Figure 1. (a) Schematic of the Atlantic Meridional Overturning Circulation (AMOC). Red ribbon indicates warm surface water, blue ribbon indicates deep cold water. Arrows show the direction of the transport. The overturning of the circulation is shown in the North Atlantic where colder, dense water sinks to the North Atlantic Deep Water (NADW). This water is transported southward via the deep ocean, to eventually upwell in the Southern Hemisphere, completing the cycle. Figure courtesy of Met Office UK, cropped to show the Atlantic sector. (b) Diagram of five-box AMOC model, adapted from Alkhayyon *et al.* (2019). Boxes are labelled as 'N' Northern Atlantic, 'T' Tropical Atlantic, 'B' North Atlantic Deep Water, 'IP' Indo-Pacific, 'S' Southern Ocean. Further details of the model used can be found in the [Supporting Information](#).

(known as bi-stability), a common feature of systems that exhibit tipping behaviour. Therefore, the AMOC could be in a stable 'on' state similar to present day but also in an 'off', collapsed state and transition between the two.

An ongoing weakening of the AMOC found in direct observational records over the last two decades substantiates the concern of a future AMOC collapse (Smeed *et al.*, 2018), although this is uncertain due to the short record. Furthermore, based on longer term sea-surface temperature observations (Caesar *et al.*, 2018) and paleo proxy records (Caesar *et al.*, 2021), it has been suggested that this weakening may have begun more than a century ago. An ongoing destabilisation of the AMOC is also indicated by studies based on early warning indicators. Those most often rely on the concept of critical slowing down, in which the time taken for the system to recover from perturbations increases as a system approaches its tipping point. Recent studies have looked for these indicators in AMOC proxy records, and do find the presence of early-warning signals (Boers, 2021; Ditlevsen and Ditlevsen, 2023). While the general detection of AMOC critical slowing down is present under a robust uncertainty analysis (Ben-Yami, Skiba, *et al.*, 2023), uncertainties from observations and AMOC fingerprints can be too large for making precise predictions (Ben-Yami, Morr, *et al.*, 2023). A physics-based early warning indicator has also suggested an ongoing destabilisation of the AMOC (van Westen *et al.*, 2024).

Bi-stability of the AMOC has been observed in conceptual models of the AMOC (Stommel, 1961; Rahmstorf, 1996; Cimatoribus *et al.*, 2014), but also in many

Earth models of intermediate complexity (Rahmstorf *et al.*, 2005), or more recently in state-of-the-art global circulation models (GCMs) (Romanou *et al.*, 2023; van Westen and Dijkstra, 2023). To investigate the possibility and consequences of an AMOC collapse, most experiments induce this by increasing the rate at which freshwater is added to the North Atlantic Ocean. This freshwater forcing can represent changes in forcing to the North Atlantic such as precipitation or ice sheet melt. It can act to weaken the overturning, which can push the system beyond a critical threshold. Recent work suggested a protocol for future hosing experiments across the latest generation of GCMs (Jackson *et al.*, 2023), which have been performed in eight different Coupled Model Intercomparison Project Phase 6 (CMIP6) models (Eyring *et al.*, 2016). Additionally, paleoclimate records show abrupt transitions of the AMOC (Broecker *et al.*, 1985), suggesting an alternative stable state could have existed in the past.

In fact, tipping in many large-scale elements of the Earth system is an active area of research, which draws from the mathematical theory of dynamical systems. From this perspective, Ashwin *et al.* (2012) have proposed different tipping mechanisms. First, bifurcation-induced tipping occurs when a system is forced past a critical threshold, and the previous stable state loses stability or ceases to exist. Consequently, the system abruptly transitions to an alternative stable state (e.g. Hawkins *et al.* (2011) and van Westen *et al.* (2024)). Second, noise-induced tipping occurs when a system is forced out of one stable regime to another by random fluctuations, despite still residing in a region of bi-stability. These random fluctuations

correspond to natural variability of the climate occurring on shorter timescales than those represented in any given model (Hasselmann, 1976). This occurs in models of varying complexity, where smaller scale (faster) processes can be modelled by a noise term (e.g. Cessi (1994) and Romanou *et al.* (2023)). Finally, rate-induced tipping occurs when a system is unable to continually adapt to a rapidly changing external forcing that causes an abrupt transition to an alternative state. Previous studies (Stocker and Schmittner, 1997; Lohmann and Ditlevsen, 2021) have shown that the rate at which freshwater forcing is added to the North Atlantic can cause the AMOC to collapse via rate-induced tipping.

In this paper, we describe and illustrate these tipping mechanisms in a conceptual model of the AMOC (Alkhayoun *et al.*, 2019; Wood *et al.*, 2019), presented in the next section. The bifurcation analysis for this model is presented for the first time, using the HadGEM3 calibration of the three-box model from Chapman *et al.* (2024). Using this model, we demonstrate the existence of bifurcation-, noise- and rate-induced tipping in subsequent sections, using exemplar freshwater forcing scenarios.

## Bifurcation analysis of a box model of the AMOC

An understanding of the AMOC and how it responds to different freshwater inputs can be gained by considering a conceptual box model of the global ocean circulation. Specifically, we consider a five-box model of the AMOC (Wood *et al.*, 2019), which is based on the same physics as the Stommel two-box model (Stommel, 1961). The box

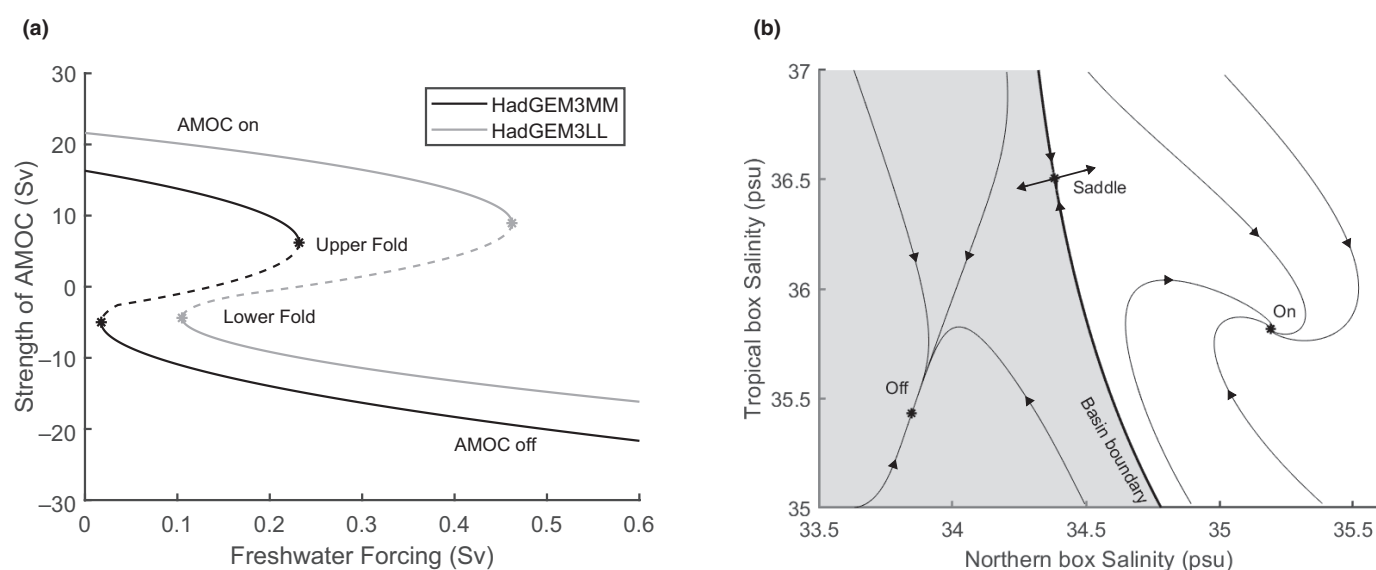


Figure 2. (a) Bifurcation diagram of three-box model, HadGEM3LL and HadGEM3MM calibration. Plotted is the circulation strength  $q$ , against the freshwater forcing. A solid line denotes a stable state, while a dashed line is unstable. The positions of the fold bifurcations are listed in Table S1 and marked as stars on the figure. Bifurcation diagrams are calculated using the AUTO software (Ermentrout, 2002). (b) Phase portrait for the HadGEM3MM calibration at 0.15 Sv 'on', 'off' and 'saddle' points are shown with arrows indicating their stability. The basin of attraction of the 'off' state is shaded grey, while the 'on' state basin is in white.

model, shown as a schematic in Figure 1(b), describes the change in salinity for each box (note temperatures are fixed). Figure 1(b) shows freshwater fluxes entering the four surface boxes. The full-model equations, along with a description of all parameters, are provided in the Supporting Information. The path of the circulation ( $q$ ) is shown in green, and arrows indicate the flow of water between the boxes. Starting in the 'T' box, water flows into the 'N' box, here overturning occurs as the denser water sinks from the 'N' box to the 'B' box. The flow of water can then take one of two different paths (Cold-water path via 'S' box, or via warm-water path, 'IP' box) before returning to the 'T' box. Consistent with model simulations (Wood *et al.*, 2019), this model can be reduced to three boxes by assuming constant salinities in the Southern and Bottom Ocean boxes,

shown in grey in Figure 1(b). The third box ('IP') can be solved by conservation of salinity, and therefore reduces the model to two dynamical boxes representing the North Atlantic Ocean and the Tropical Ocean.

The model switches between two different regimes of equation depending on the sign of the strength of the circulation. When the circulation strength drops below zero, the new equations describe a reversal of the circulation, which would effectively switch the AMOC from its current 'on' state to an 'off' state. The strength of the circulation,  $q$ , is governed by the following equation:

$$q = \lambda(\alpha(T_S - T_N) + \beta(S_N - S_S)), \quad (1)$$

where  $S$  and  $T$  are the salinities and temperatures of the two boxes indicated by

the subscripts 'N, S' for the Northern and Southern boxes. Note the strength of the circulation depends on only one dynamic state variable, the salinity in the Northern box,  $S_N$ . The strength of the circulation depends on gradients of salinity and temperature, with differing signs and magnitude of influence. For the remaining parameters,  $T_N$ ,  $T_S$ ,  $\lambda$ ,  $\alpha$  and  $\beta$ , we use values calibrated to HadGEM3-GC3.1-LL and HadGEM3-GC3.1-MM (abbreviated to HadGEM3LL and HadGEM3MM for the low and medium resolutions respectively), which are explained and given in Chapman *et al.* (2024). The advantage of calibrating to a higher order GCM is that the box model should much more closely represent the dynamics expected in the real-world AMOC, as these models are of much higher resolution. Here we use the calibration to HadGEM3 from Chapman

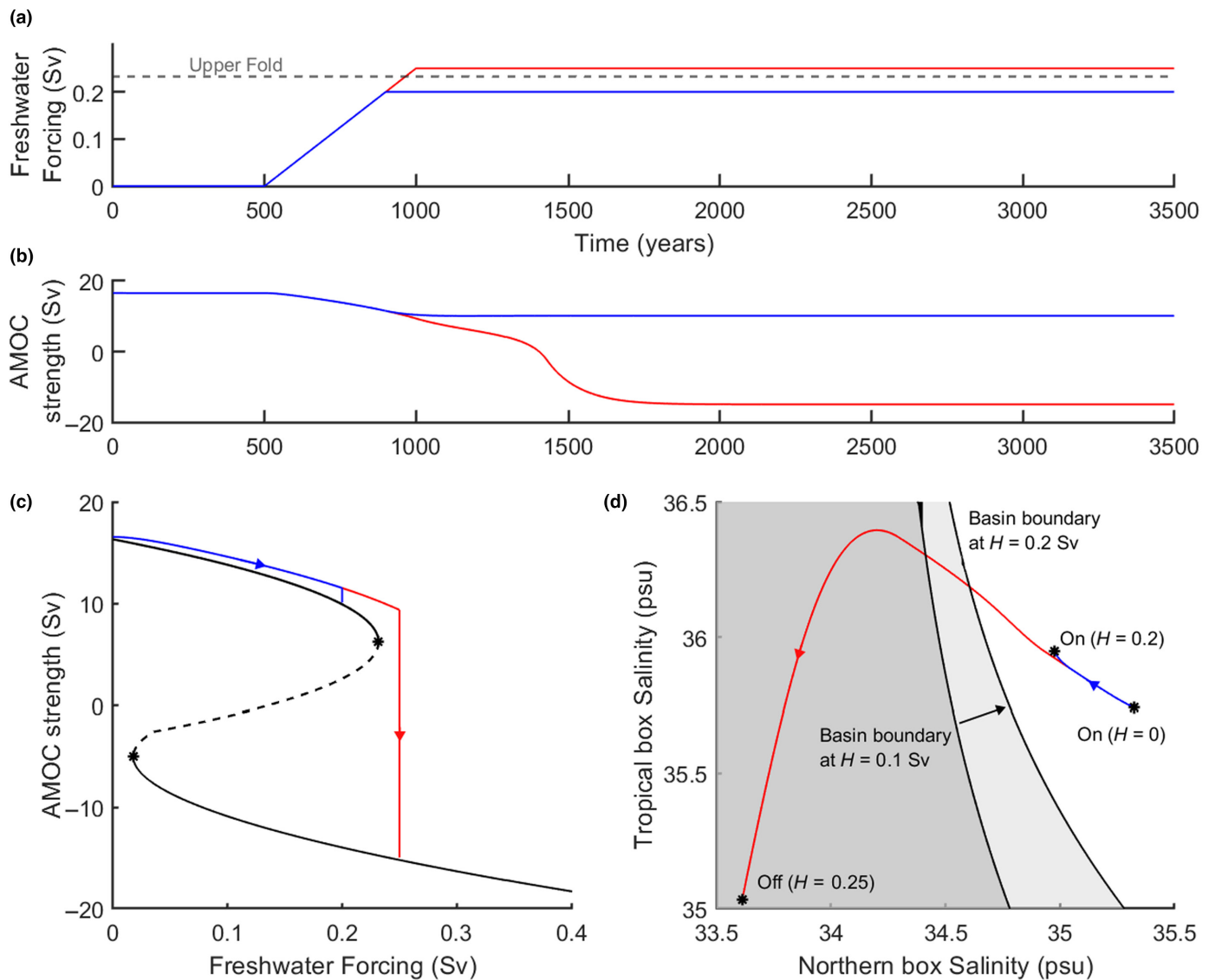


Figure 3. Bifurcation-induced tipping in the three-box AMOC model calibrated to HadGEM3MM. Red line shows a scenario that has been forced beyond the Upper Fold and tips to the 'off' state. Blue line is a scenario where forcing stops before the Fold and remains in the 'on' state. (a) Plot of freshwater forcing functions applied. Red increases to 0.25Sv, blue to 0.2Sv. (b) Time series of AMOC strength. (c) Plot of AMOC strength for the scenarios plotted over the bifurcation diagram in black. (d) Phase portrait of salinities. Both trajectories start at 'On ( $H=0$ Sv)'. Black curves show the basin boundaries for different levels of freshwater forcing, and the black arrow shows how the boundary shifts with increasing forcing. Shading indicates basin of attraction, initial conditions that converge to 'off' are shaded grey, the 'on' state is in white. Light grey still indicates the 'off' state, at the higher forcing level.

*et al.* (2024), and present a bifurcation analysis using these model parameters. We use two calibrations here to compare the difference that model resolution can have on the bifurcation structure.

Figure 2(a) shows the bifurcation diagrams for these calibrations (Chapman *et al.*, 2024) of the three-box AMOC model, and allows us to identify equilibrium branches (i.e. the position of equilibrium solutions), their stability and the positions of bifurcation points. Freshwater forcing, measured in Sverdrups (Sv) (a volumetric flow rate with a Sv approximately corresponding to  $1 \times 10^6 \text{m}^3 \text{s}^{-1}$ ), acts as the control parameter, while the resulting circulation is characterised by the strength of the AMOC. We find that the bifurcation structure is qualitatively the same for the two calibrations, taking the classical form of a double fold bifurcation, which is the mathematical archetype of a tipping point.

A double-fold bifurcation takes the form of an S-shape curve (as in Figure 2a), with two saddle-node bifurcations that mark the collision of the saddle (black dashed curve, unstable) with a stable node (black solid curve). The upper stable branch corresponds to the AMOC 'on' state, while the lower stable branch is the AMOC 'off' state, as labelled in Figure 2(a). We compare this result to previous studies (Alkhayyon *et al.*, 2019) in a later section. Shown in Figure 2(b) is the phase portrait at  $H=0.15\text{Sv}$  for the HadGEM3MM calibration. The boundary separates the basins of attraction (the set of points that converge to a stable state) for the two stable states. Some sample trajectories in the phase space are plotted.

There are some important quantitative differences to highlight between the bifurcation diagrams for the calibrations. Firstly, the Upper Fold bifurcation for the low-

resolution calibrated model is at a higher level of freshwater forcing ( $\sim 0.55\text{Sv}$  for -LL compared to  $\sim 0.2\text{Sv}$  for -MM). This means that the AMOC is much more resilient, and therefore more freshwater is required for the AMOC to experience tipping to the 'off' state. A recent study (Jackson *et al.*, 2023) suggests that the higher resolution full HadGEM3 model has an earlier threshold (compared to the lower resolution HadGEM3 model), which agrees with the result we find.

The Lower Fold bifurcation is similarly at a higher freshwater forcing level for the low resolution compared with the medium resolution calibration. However, the difference is not as large as for the Upper Fold, and therefore the region of bi-stability (where the AMOC 'on' and 'off' states coexist) is also greater for the low-resolution calibration. This large difference in the position of the tipping threshold highlights the uncertainty

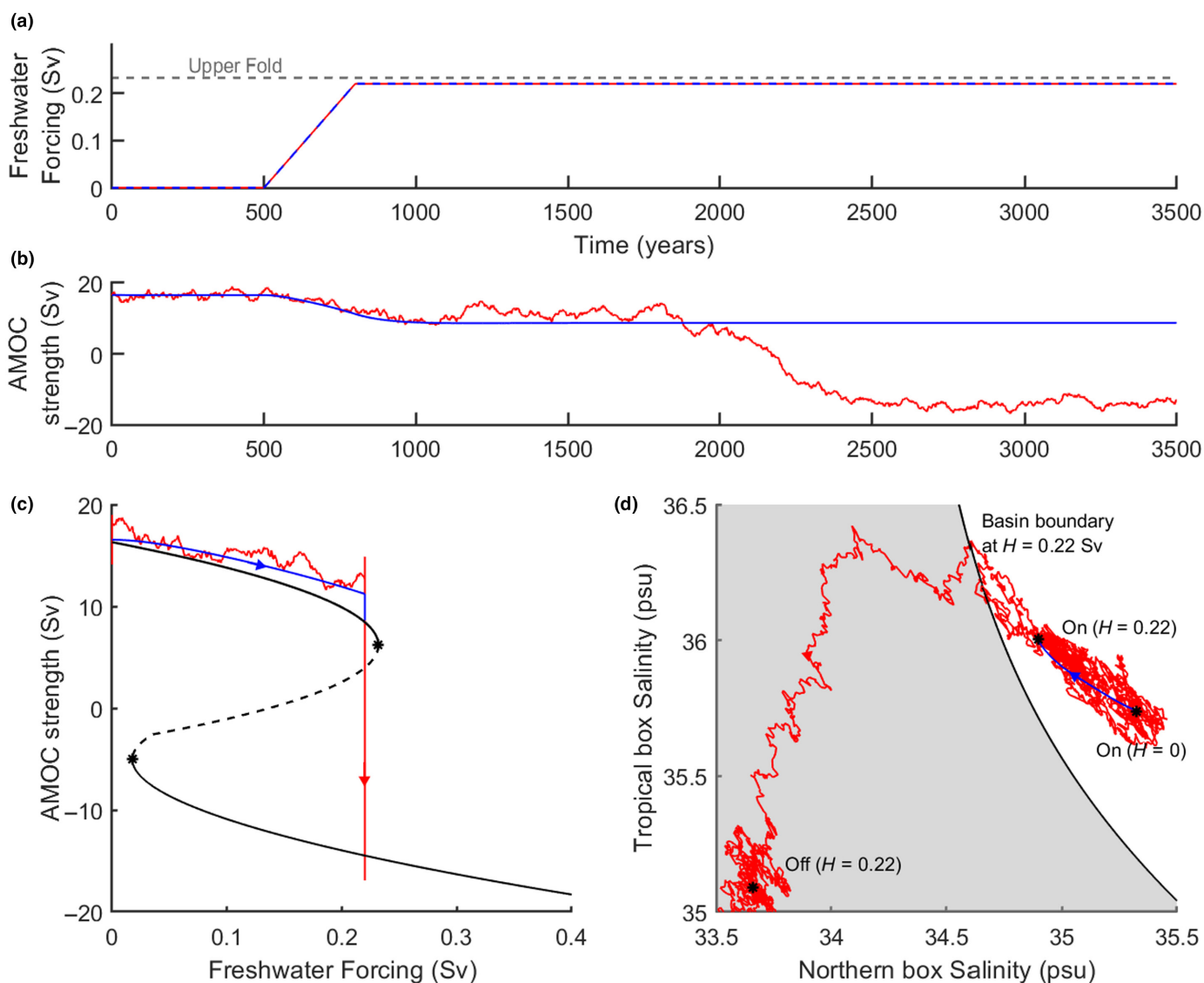


Figure 4. Noise-induced tipping in HadGEM3MM calibration with identical forcing increasing to 0.22Sv. Red line forced with 10 times the estimated noise for HadGEM3MM from CMIP6 pre-industrial control runs, and blue line no noise. (a) Freshwater forcing function applied (identical for both scenarios). The position of the Upper Fold is shown as a black dashed line. (b) Time series of AMOC strength. (c) Plot of AMOC strength for the scenarios plotted over the bifurcation diagram in black. (d) Phase portrait of salinities. Both trajectories start at 'On ( $H=0\text{Sv}$ ): The black line shows the basin boundary at ' $H=0.22\text{Sv}$ '.

in AMOC tipping. We suggest that the difference in the calibrations is primarily due to the different resolutions of the models, and one would need to consider many different calibrations across different GCMs to fully quantify this. However, similar results are seen in the full-scale climate model, HadGEM3, in Jackson *et al.* (2023). The lower resolution model, HadGEM3LL, appears to show greater resilience upon increasing the freshwater forcing than the higher resolution model, HadGEM3MM. These runs however, are relatively short in duration and so determining the possible change in the tipping threshold location is challenging.

In the subsequent sections, we will focus our analyses on the calibration for the medium resolution model, HadGEM3MM.

## Bifurcation-induced tipping

One scenario that can lead to tipping of the AMOC is via bifurcation-induced tipping. In this case, the 'on' state is lost by increasing the freshwater forcing beyond the Upper Fold bifurcation, and now the AMOC 'off' state is the only remaining stable state.

This behaviour can be illustrated by considering two distinct freshwater forcing profiles that both follow a linear ramp. The rate of increase is the same, but they are applied up to different freshwater forcing levels (see blue and red curves in Figure 3a). We observe that the blue forcing scenario maintains the AMOC in an 'on' state, while the red forcing scenario results in an AMOC collapse (Figure 3b). This can be explained by Figure 3(c), the red trajectory is forced beyond the position of the Upper Fold, meaning that the upper stable branch has disappeared. Consequently, the AMOC collapses to the lower stable branch, which is now the only existing attracting state and corresponds to a reversal of the circulation. In contrast, for the blue trajectory the forcing stops before the Upper Fold and therefore remains on the upper stable branch.

Figure 3(d) displays the trajectories in the phase plane of the system projected in two dimensions, namely the salinity in the Tropics against the salinity in the North Atlantic. For zero freshwater forcing ( $H=0\text{Sv}$ ), only the 'on' state exists as a stable equilibrium and likewise above the Upper Fold ( $H=0.25\text{Sv}$ ) only the stable 'off' state exists. However, for a range of intermediate freshwater forcing values the model is bi-stable, where a basin boundary separates their basins of attraction – sets of initial conditions that converge to the corresponding stable state. The basin boundary is plotted in black for two values of freshwater forcing to indicate how the boundary moves upon increasing the forcing. Basin of attraction for the 'off' state is shaded in grey. Here, the 'on' state and

basin boundary move closer together (they collide and disappear at the Upper Fold) upon increasing the forcing. However, by stopping the forcing before the Upper Fold, the blue trajectory always remains inside the basin of attraction of the 'on' state, and therefore avoids tipping to the 'off' state. In contrast, the red scenario forces the model beyond the Upper Fold, meaning that the basin of attraction of the 'off' state becomes the entire region and therefore tipping to the 'off' state ensues.

## Noise-induced tipping

Noise-induced tipping occurs when random perturbations can force a system across a basin boundary. To demonstrate noise-induced tipping, we transform the three-box model into a stochastic model by introducing additive white noise, which is parameterised by prescribed noise amplitudes that have been estimated from HadGEM3MM (Chapman *et al.*, 2024). This noise could correspond to unresolved processes (such as small-scale ocean currents), which are smaller or on faster time scales than the resolution of the box model. To isolate the effect of noise, we increase the freshwater forcing close to, but not past, the Upper Fold. We also raise the noise amplitudes above those estimated from the GCM, without overshadowing the system's dynamics (i.e. stable states can still be identified), as in Chapman *et al.* (2024).

Figure 4 shows an example of noise-induced tipping, where the same forcing is applied to both scenarios, see Figure 4(a). Both scenarios are forced to  $0.22\text{Sv}$ , which is below the position of the Upper Fold (see Table S1), and before the bifurcation. The AMOC strength decreases due to the

increase in the control parameter, but without noise there is no abrupt AMOC collapse because the forcing stops before the bifurcation is crossed. However, when adding noise, the AMOC can collapse roughly 1000 years after the forcing is stopped, see Figure 4(b).

These same trajectories are shown overlaid on the bifurcation diagram in Figure 4(c), where we see that the collapse happens without crossing the Upper Fold bifurcation. Figure 4(d) shows the trajectories in phase space. We see that both scenarios follow the moving 'on' state upon the forcing changing. Once the forcing stops, the red trajectory continues to fluctuate around the 'On ( $H=0.22\text{Sv}$ )' state. After a period of time, the system moves towards the basin boundary, caused by the fluctuations. Once at the boundary, the probability of tipping increases as one further 'kick', may be sufficient to cross the basin boundary, and consequently tip the system to the 'off' state. Alternatively, the noise may push the system back towards the 'on' state and reduce the chance of a tipping, or result in only a very short excursion over the basin boundary. Consequently, we must rely on a probabilistic approach to critical transitions, such as Monte Carlo simulations (Chapman *et al.*, 2024). Figure 4 displays a realisation of noise that tips, while other noise realisations may not tip.

## Rate-induced tipping

A third mechanism, rate-induced tipping, occurs when a system is forced too quickly, and without crossing any critical thresholds, abruptly transitions to an alternative state. In this case, the system is unable to track the moving, original stable state and consequently falls outside its basin of attraction, and therefore tipping follows.

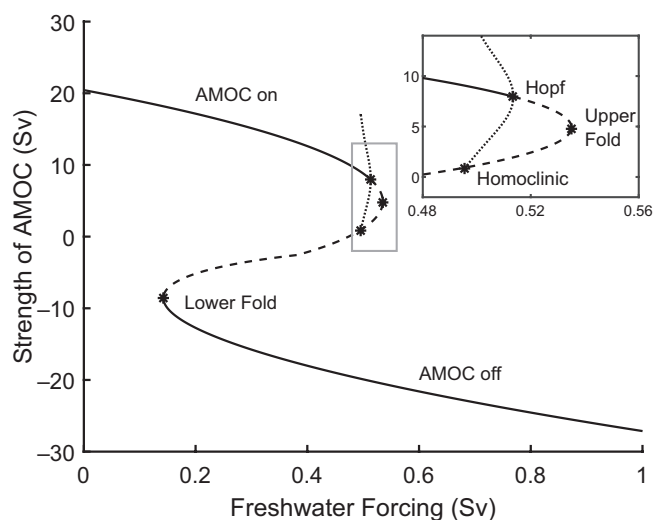


Figure 5. Bifurcation diagram for the three-box model calibrated to HadGEM3MM with the Southern box wind flux parameter from Chapman *et al.* (2024) divided by five. Solid black corresponds to a stable branch, a dashed line is an unstable branch. The dotted line shows the limit cycle. All bifurcation points are labelled as well as the homoclinic point (where the limit cycle meets the saddle). The positions of the bifurcation points are shown in Table S1.

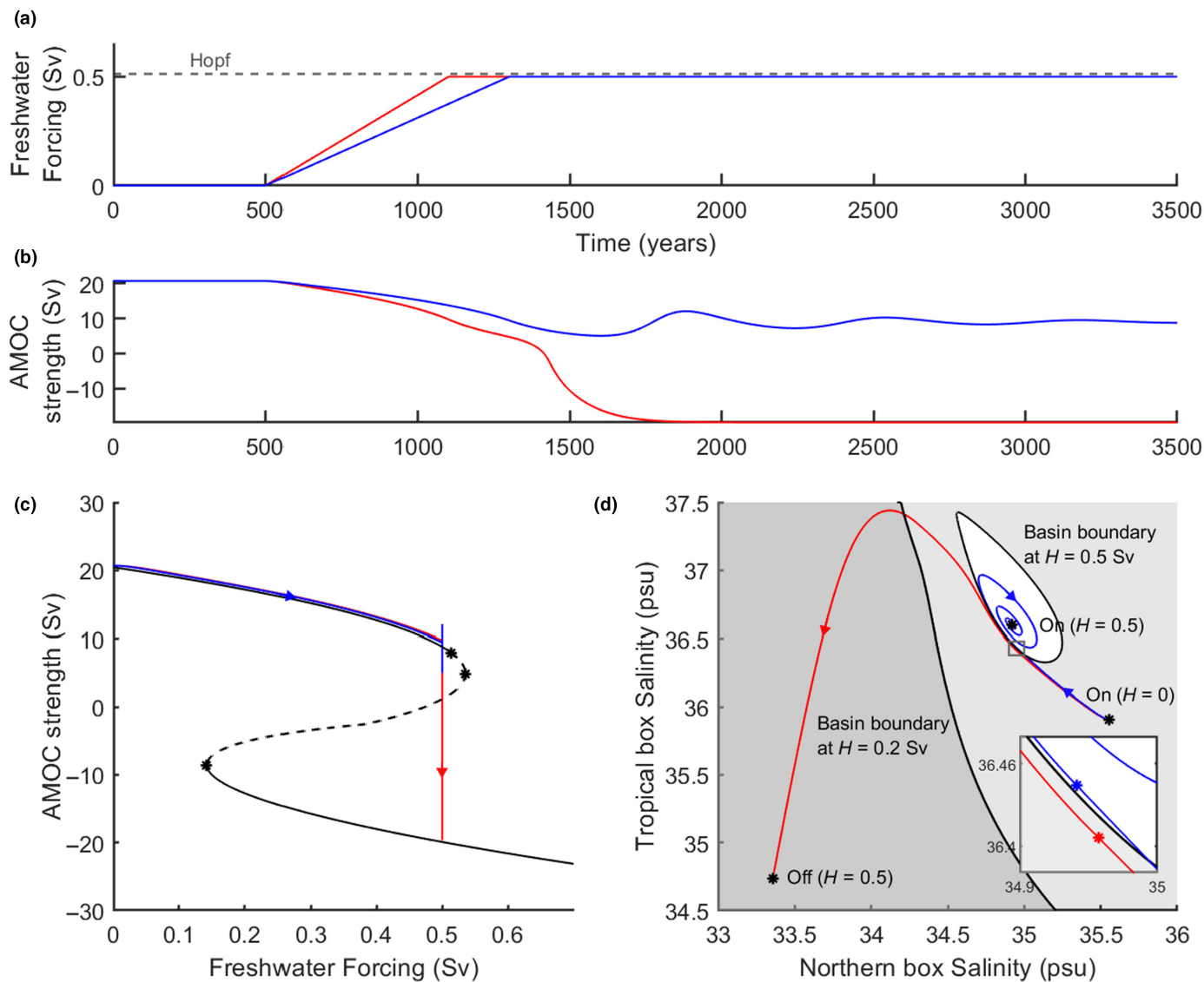


Figure 6. Rate-induced tipping with HadGEM3MM calibration and the Southern box wind flux parameter from Chapman *et al.* (2024) divided by five. Both scenarios are forced to the same level but stop before the Hopf bifurcation. (a) Freshwater forcing functions applied. Position of the Hopf point is shown in black dashed line. Freshwater forcing is increased to 0.5 Sv in both scenarios. In the red scenario, freshwater is increased over 600 years, while in the blue scenario it is increased over 800 years. (b) Time series of AMOC strength. (c) Plot of AMOC strength for the scenarios plotted over the bifurcation diagram in black. The limit cycle has been removed for clarity. (d) Phase portrait of salinities, both scenarios start from 'On ( $H=0$  Sv)'. Basin boundary at ' $H=0.5$  Sv' is shown, which features an unstable limit cycle – black ellipse. Star markers indicate position of trajectory when the freshwater forcing stops in the respective scenarios, also in the insert. Dark grey shading indicates basin of attraction of 'off' state at  $H=0.2$  Sv, light grey is the basin at 0.5 Sv and white the remaining basin for the 'on' state at this stabilised forcing level.

The original calibration of the three-box model (Alkhayouon *et al.*, 2019), was found to facilitate rate-induced tipping. However, the HadGEM3MM calibration does not feature basin instability (i.e. the initial 'on' state remains within all future basins of attraction of the 'on' state), as seen in Figure 3(d). The lack of basin instability, and numerical simulations, suggest that rate-induced tipping is not possible. The mathematical proof required to show this (Kiers and Jones, 2020) however, is outside the scope of this article.

A key difference from the original calibration, is that the HadGEM3 calibration does not feature what is known as a sub-critical Hopf bifurcation. At the sub-critical Hopf bifurcation (in the original calibration) an

unstable periodic solution ends and the stability of the equilibrium branch changes from stable to unstable for increasing the freshwater forcing. In such a configuration, basin instability arises, which has previously been shown to be a sufficient condition for rate-induced tipping (Ritchie *et al.*, 2023).

We find that the sub-critical Hopf bifurcation re-emerges if the value of the Southern box wind flux parameter, given in Chapman *et al.* (2024), is reduced by a factor of five, see Figure 5. Note that the wind flux parameters are the only parameters that are not obtained directly from HadGEM3MM. Instead, they must be diagnosed from the gyre salt transport across the box boundaries, and consequently carry a higher uncertainty (Wood *et al.*, 2019). The

presence of the Hopf bifurcation means that bifurcation-induced tipping occurs earlier than initially expected, due to the loss of stability at the Hopf instead of the Upper Fold. Furthermore, the basin of attraction of the 'on' state greatly reduces in size resulting in basin instability.

The response of the AMOC to two different freshwater forcing scenarios in this modified HadGEM3 calibration is given in Figure 6. The freshwater forcing scenarios, Figure 6(a), are forced to the same level but at different rates. The forcing does not reach any bifurcation point, so will not induce bifurcation tipping. If the change in freshwater forcing is sufficiently slow (blue trajectory), then the AMOC will remain in its original 'on' state (Figure 6b). On the other

hand, if the freshwater forcing increases too quickly, such as for the red trajectory, then the AMOC collapses to its 'off' state. In Figure 6(c) the trajectories are overlaid on top of the bifurcation diagram. The red trajectory shows unexpected behaviour, tipping (without any noise disturbances) from the upper stable branch to the lower branch, close to but before the Hopf, and long before the Upper Fold.

Figure 6(d) helps unravel this initially counter-intuitive behaviour. Note that the basin boundary of the 'on' state, at  $H=0.55Sv$ , now encloses a small, finite region. We can see from the insert in Figure 6(d), that the blue trajectory is inside the future basin of attraction of the 'on' state, at the point where the forcing stops, indicated by the blue star. The system subsequently spirals (due to the unstable limit cycle emanating from the sub-critical Hopf bifurcation) back in to the AMOC 'on' state.

However, note that the initial starting position is outside the basin of attraction of the 'on' state at the final level of freshwater forcing. Therefore, the system is basin unstable, and thus for a sufficiently fast change in the freshwater forcing, such as the red trajectory, the AMOC will undergo rate-induced tipping. As shown by the red marker in the insert, at the point when the freshwater forcing stops, the system is outside the basin of attraction of the 'on' state. Therefore, it tips to the 'off' state. Between the two rates displayed there will be a critical rate, which separates tracking the 'on' state and rate-induced tipping to the 'off' state.

## Conclusion

The AMOC is an important part of the global ocean circulation and therefore it is important to understand how it may respond under anthropogenic forcing, including the possibility of an abrupt, non-linear response occurring at a critical threshold of freshwater forcing (tipping point). We have presented a conceptual three-box dynamical AMOC model, calibrated against a GCM, and have shown examples of bifurcation-, noise- and rate-induced tipping. We find that increasing freshwater forcing beyond a determined level or natural variability (represented by noise) can result in an AMOC collapse via bifurcation- and noise-induced tipping, respectively. While the AMOC collapse via bifurcation-induced tipping is robust for different model calibrations, the determined level of freshwater forcing required to cross the tipping threshold (represented by a fold bifurcation) varies considerably based on the calibration of the model. This will have important consequences for designing mitigation pathways, such as overshoot scenarios (Ritchie *et al.*, 2021) that avoid tipping the AMOC.

Moreover, we found an example of an adjusted parameter configuration that yields a Hopf bifurcation. Under this configuration, the model features basin instability, making rate-induced tipping another plausible mechanism. Therefore, additional calibrations of this box model (for example, to further CMIP6 models), are needed to assess the viability of rate-induced tipping as a possible tipping mechanism for the AMOC. This is particularly pertinent given the scarcity of rate-induced tipping studies of the AMOC with high complexity models (Lohmann and Ditlevsen, 2021). Results of the box model under these additional calibrations can also be compared against GCM runs, such as van Westen *et al.* (2024). Developing a collection of calibrations (to different CMIP6 models) would allow for an ensemble of box model runs, which could capture some of the spread in behaviour seen in CMIP6 (Jackson *et al.*, 2023). This would provide opportunity to generate a greater understanding of the long term behaviour of the AMOC under a variety of different forcing scenarios.

## Acknowledgements

R.C. conducted this research as part of an EPSRC CASE PhD studentship with the Met Office and the University of Exeter grant agreement number EP/T518049/1. S.S. acknowledges funding from the European Union's Horizon 2020 research and innovation programme under the Marie Skłodowska-Curie Actions, grant agreement number 956170 (CriticalEarth), from the European Union's Horizon 2020 programme. P.D.L.R. was supported by the Optimal High Resolution Earth System Models for Exploring Future Climate Changes (OptimESM) project, grant agreement number 101081193 from the European Union's Horizon (Climate, Energy and Mobility). Thanks to Peter Ashwin and Richard Wood for their supervision and helpful comments on this work. Many thanks to Maya Ben-Yami for commentary on critical slowing down. Thank you to Hassan Alkhayuon for permission to reprint his results in Table S1. For the purpose of open access, the author has applied a Creative Commons Attribution (CC BY) licence to any Author Accepted Manuscript version arising from this submission.

## Author contributions

**Ruth Chapman:** Project administration; visualization; investigation; formal analysis; software; conceptualization; writing – original draft; writing – review and editing. **Sacha Sinet:** Writing – original draft; writing – review and editing; conceptualization. **Paul D. L. Ritchie:** Conceptualization; writing – original draft; writing – review and editing; software; formal analysis; investigation.

## Data availability statement

No original data were created in this work.

## Supporting Information

Additional supporting information may be found online in the Supporting Information section at the end of the article.

**Data S1.**

## References

- Alkhayuon H, Ashwin P, Jackson LC** *et al.* 2019. Basin bifurcations, oscillatory instability and rate-induced thresholds for Atlantic Meridional Overturning Circulation in a global oceanic box model. *Proc. Math. Phys. Eng. Sci.* **475**(2225): 20190051. <https://doi.org/10.1098/rspa.2019.0051>
- Armstrong McKay DI, Staal A, Abrams JF** *et al.* 2022. Exceeding 1.5°C global warming could trigger multiple climate tipping points. *Science* **377**(6611): eabn7950. <https://doi.org/10.1126/science.abn7950>
- Ashwin P, Wieczorek S, Vitolo R** *et al.* 2012. Tipping points in open systems: bifurcation, noise-induced and rate-dependent examples in the climate system. *Philos. Trans. R. Soc. A Math. Phys. Eng. Sci.* **370**(1962): 1166–1184. <https://doi.org/10.1098/rsta.2011.0306>
- Bellomo K, Angeloni M, Corti S** *et al.* 2021. Future climate change shaped by inter-model differences in Atlantic Meridional Overturning Circulation response. *Nat. Commun.* **12**: 3659. <https://doi.org/10.1038/s41467-021-24015-w>
- Ben-Yami M, Morr A, Bathiany S** *et al.* 2023. Uncertainties too large to predict tipping times of major earth system components (pre-print). <https://doi.org/10.48550/arXiv.2309.08521>
- Ben-Yami M, Skiba V, Bathiany S** *et al.* 2023. Uncertainties in critical slowing down indicators of observation-based fingerprints of the Atlantic Overturning Circulation. *Nat. Commun.* **14**(8344): 1–11. <https://doi.org/10.1038/s41467-023-44046-9>
- Boers N.** 2021. Observation-based early-warning signals for a collapse of the Atlantic Meridional Overturning Circulation. *Nat. Clim. Chang.* **11**(8): 680–688. <https://doi.org/10.1038/s41558-021-01097-4>
- Broecker W, Peteet D, Rind D.** 1985. Does the ocean-atmosphere system have more than one stable mode of operation? *Nature* **315**(6014): 21–26. <https://doi.org/10.1038/315021a0>
- Caesar L, McCarthy GD, Thornalley DJR** *et al.* 2021. Current Atlantic Meridional Overturning Circulation weakest in last millennium. *Nat. Geosci.* **14**(3): 118–120. <https://doi.org/10.1038/s41561-021-00699-z>
- Caesar L, Rahmstorf S, Robinson A** *et al.* 2018. Observed fingerprint of a weakening Atlantic Ocean Overturning Circulation. *Nature* **556**(7700): 191–196. <https://doi.org/10.1038/s41586-018-0006-5>

- Cessi P.** 1994. A simple box model of stochastically forced thermohaline flow. *J. Phys. Oceanogr.* **24**(9): 1911–1920. [https://doi.org/10.1175/1520-0485\(1994\)024<1911:ASBMOS>2.0.CO;2](https://doi.org/10.1175/1520-0485(1994)024<1911:ASBMOS>2.0.CO;2)
- Chapman R, Ashwin P, Wood R et al.** 2024. Quantifying risk of a noise-induced AMOC collapse from northern and tropical Atlantic ocean variability. *arXiv preprint*. <https://doi.org/10.48550/arXiv.2405.10929>
- Cimatoribus AA, Drijfhout SS, Dijkstra HA.** 2014. Meridional overturning circulation: stability and ocean feedbacks in a box model. *Clim. Dyn.* **42**(1): 311–328. <https://doi.org/10.1007/s00382-012-1576-9>
- Dekker MM, von der Heydt AS, Dijkstra HA.** 2018. Cascading transitions in the climate system. *Earth Syst. Dyn.* **9**(4): 1243–1260. <https://doi.org/10.5194/esd-9-1243-2018>
- Ditlevsen P, Ditlevsen S.** 2023. Warning of a forthcoming collapse of the Atlantic Meridional Overturning Circulation. *Nat. Commun.* **14**(1): 4254. <https://doi.org/10.1038/s41467-023-39810-w>
- Ermentrout B.** 2002. Simulating, Analyzing, and Animating Dynamical Systems. Society for Industrial and Applied Mathematics: Philadelphia. <https://doi.org/10.1137/1.9780898718195>
- Eyring V, Bony S, Meehl GA et al.** 2016. Overview of the Coupled Model Intercomparison Project Phase 6 (CMIP6) experimental design and organization. *Geosci. Model Dev.* **9**(5): 1937–1958. <https://doi.org/10.5194/gmd-9-1937-2016>
- Hasselmann K.** 1976. Stochastic climate models Part I. Theory. *Tellus* **28**(6): 473–485. <https://doi.org/10.1111/j.2153-3490.1976.tb00696.x>
- Hawkins E, Smith RS, Allison LC et al.** 2011. Bistability of the Atlantic Overturning Circulation in a global climate model and links to ocean freshwater transport. *Geophys. Res. Lett.* **38**(10): L10605. <https://doi.org/10.1029/2011GL047208>
- Jackson LC, Alastrué De Asenjo E, Bellomo K et al.** 2023. Understanding AMOC stability: the North Atlantic Hosing Model Intercomparison Project. *Geosci. Model Dev.* **16**(7): 1975–1995. <https://doi.org/10.5194/gmd-16-1975-2023>
- Jackson LC, Kahana R, Graham T et al.** 2015. Global and European climate impacts of a slowdown of the AMOC in a high resolution GCM. *Clim. Dyn.* **45**(11–12): 3299–3316. <https://doi.org/10.1007/s00382-015-2540-2>
- Kiers C, Jones CK.** 2020. On conditions for rate-induced tipping in multi-dimensional dynamical systems. *J. Dyn. Diff. Equat.* **32**(1): 483–503. <https://doi.org/10.1007/s10884-019-09730-9>
- Klose AK, Wunderling N, Winkelmann R et al.** 2021. What do we mean, 'tipping cascade'? *Environ. Res. Lett.* **16**(12): 125011. <https://doi.org/10.1088/1748-9326/ac3955>
- Lohmann J, Ditlevsen PD.** 2021. Risk of tipping the overturning circulation due to increasing rates of ice melt. *Proc. Natl. Acad. Sci.* **118**(9): e2017989118. <https://doi.org/10.1073/pnas.2017989118>
- Rahmstorf S.** 1996. On the freshwater forcing and transport of the Atlantic thermohaline circulation. *Clim. Dyn.* **12**(12): 799–811. <https://doi.org/10.1007/s0038200050144>
- Rahmstorf S, Crucifix M, Ganopolski A et al.** 2005. Thermohaline circulation hysteresis: a model intercomparison. *Geophys. Res. Lett.* **32**(23): L23605. <https://doi.org/10.1029/2005GL023655>
- Ritchie PD, Alkhayuon H, Cox PM et al.** 2023. Rate-induced tipping in natural and human systems. *Earth Syst. Dyn.* **14**(3): 669–683. <https://doi.org/10.5194/esd-14-669-2023>
- Ritchie PD, Clarke JJ, Cox PM et al.** 2021. Overshooting tipping point thresholds in a changing climate. *Nature* **592**(7855): 517–523.
- Romanou A, Rind D, Jonas J et al.** 2023. Stochastic bifurcation of the north Atlantic circulation under a mid-range future climate scenario with the NASA-GISS ModelE. *J. Clim.* **36**(18): 6141–6161. <https://doi.org/10.1175/JCLI-D-22-0536.1>
- Sarmiento J, Le Quéré C.** 1996. Oceanic carbon dioxide uptake in a model of century-scale global warming. *Science* **274**(5291): 1346–1350. <https://doi.org/10.1126/science.274.5291.1346>
- Seager R, Battisti DS, Yin J et al.** 2002. Is the gulf stream responsible for Europe's mild winters? *Q. J. R. Meteorol. Soc.* **128**(586): 2563–2586. <https://doi.org/10.1256/qj.01.128>
- Sinet S, von der Heydt AS, Dijkstra HA.** 2023. AMOC stabilization under the interaction with tipping polar ice sheets. *Geophys. Res. Lett.* **50**(2): e2022GL100305. <https://doi.org/10.1029/2022GL100305>
- Smeed DA, Josey SA, Beaulieu C et al.** 2018. The north Atlantic ocean is in a state of reduced overturning. *Geophys. Res. Lett.* **45**(3): 1527–1533. <https://doi.org/10.1002/2017GL076350>
- Stocker T, Schmittner A.** 1997. Influence of CO<sub>2</sub> emission rates on the stability of the thermohaline circulation. *Nature* **388**: 862–865. <https://doi.org/10.1038/42224>
- Stommel H.** 1961. Thermohaline convection with two stable regimes of flow. *Tellus* **13**(2): 224–230. <https://doi.org/10.1111/j.2153-3490.1961.tb00079.x>
- van Westen RM, Dijkstra HA.** 2023. Asymmetry of AMOC hysteresis in a state-of-the-art global climate model. *Geophys. Res. Lett.* **50**(22): e2023GL106088. <https://doi.org/10.1029/2023GL106088>
- van Westen RM, Kliphuis M, Dijkstra HA.** 2024. Physics-based early warning signal shows that AMOC is on tipping course. *Sci. Adv.* **10**(6): eadk1189. <https://doi.org/10.1126/sciadv.adk1189>
- Wood R, Rodríguez JM, Smith RS et al.** 2019. Observable, low-order dynamical controls of thresholds of the Atlantic Meridional Overturning Circulation. *Clim. Dyn.* **53**(11): 6815–6834. <https://doi.org/10.1007/s00382-019-04956-1>
- Wunderling N, Donges JF, Kurths J et al.** 2021. Interacting tipping elements increase risk of climate domino effects under global warming. *Earth Syst. Dyn.* **12**(2): 601–619. <https://doi.org/10.5194/esd-12-601-2021>
- Wunderling N, von der Heydt A, Aksenov Y et al.** 2023. Climate tipping point interactions and cascades: a review. *EGU sphere.* **2023**: 1–45. <https://doi.org/10.5194/egusphere-2023-1576>

Correspondence to: R. Chapman  
[ruth.chapman@nbi.ku.dk](mailto:ruth.chapman@nbi.ku.dk)

© 2024 The Author(s). Weather published by John Wiley & Sons Ltd on behalf of Royal Meteorological Society.

This is an open access article under the terms of the [Creative Commons Attribution License](https://creativecommons.org/licenses/by/4.0/), which permits use, distribution and reproduction in any medium, provided the original work is properly cited.

doi: 10.1002/wea.7609